Thermal studies on the decomposition of 3,5-dinitrobenzoic acid and lead salts of 3,5-dinitrobenzoic acid

G. Om Reddy and K.S. Ravikumar

INBRI, Div. of IDL Chemicals Ltd., P.B. No. 397, Malleswaram, Bangalore-560 003 (India)

(Received 31 July 1991)

Abstract

A detailed thermal study was carried out on 3,5-dinitrobenzoic acid and the normal and basic lead salts of 3,5-dinitrobenzoic acid using differential scanning calorimetry and thermogravimetry. The thermal sensitivity increases with increase in basicity. The kinetics of thermal decomposition suggest different decomposition mechanisms for the normal and basic salts of 3,5-dinitrobenzoic acid. Thus, Pb–O bond breakage controls the decomposition of the basic salt whereas C–NO$_2$ bond breakage determines the decomposition mechanism of the normal salt. Mass spectral study indicated some unexpected ions due to the explosion of lead salts of 3,5-dinitrobenzoic acid.

INTRODUCTION

3,5-Dinitrobenzoic acid (3,5-DNBA) is a raw material for the manufacture of initiatory explosive [1]. The lead salt of 3,5-DNBA has proved to be a much safer initiatory explosive compared with the lead salt of styphnic acid (lead styphnate). A mixture of the lead salt of 3,5-DNBA and lead azide (LA) was found to be safer than a mixture of lead styphnate and LA. The power of the lead salt of 3,5-DNBA is 35% of that of trinitrotoluene (TNT) and its sensitivity is about the same as that of TNT. Its thermal stability is very good and its hygroscopicity at 90% relative humidity is negligible. Brun [2,3] and Burdett and Calhoun [4] recommended the use of this salt as an ingredient of priming compositions. 3,5-DNBA can be converted into its basic lead salt by reacting sodium salt of 3,5-DNBA with excess lead nitrate solution. Friederich [5] obtained a patent on basic lead 3,5-DNBA as an ingredient of primary compositions.

Because its sensitivity to heat, friction, impact and electrostatic charge is very low compared with the highly sensitive lead styphnate, it appears to be a better candidate for primary compositions in terms of safety.

Correspondence to: G. Om Reddy, INBRI, Division of IDL Chemicals Ltd., P.B. 397, Malleswaram, Bangalore-560 003, India.

The literature reveals no reports of the thermal decomposition characteristics of the lead salt of 3,5-DNBA using differential scanning calorimetry (DSC) and thermogravimetry (TG) techniques. Fogelzang et al. [6] have studied the combustion rates of the potassium, lead and ammonium salts of 3,5-DNBA. Differential thermal analysis (DTA) was used by Kaderabek et al. [7] to study the thermal stability of 3,5-DNBA, dinitrophenol and 3,5-dinitroaniline, and they concluded that phenols and anilines are less stable than the acid. Reaction thermal analysis (RTA) was carried out on nitroaromatic acids by Frank et al. [8], who discussed the catalytic effects of alkali and cupric carbonate on the decomposition of such acids. Dorsett and Nagy [9] studied the explosive properties of 3,5-DNBA dust. Electron impact negative ion mass spectrometry of 3,5-DNBA was carried out by Bowie [10] and photodissociation of ions generated by the soft ionisation technique was reported by Welch et al. [11]. In the absence of DSC and TG studies on the lead salts of 3,5-DNBA, it is therefore warranted to study the thermal sensitivity, thermal decomposition and kinetics of thermal decomposition of 3,5-DNBA and lead salts of 3,5-DNBA using the above techniques. We have reported earlier our mass spectral studies on the lead salts of dinitroresorcinol [12] and picramic acid [13]. In this paper, we discuss a similar study extended to 3,5-DNBA and the lead salts of 3,5-DNBA. Two types of lead salts are known, depending on the preparation conditions: (1) the normal lead salt and (2) the basic lead salt. The basic lead salt of 3,5-DNBA exhibits better flowing properties and higher density compared with the normal lead salt. First we discuss the thermal behaviour of 3,5-DNBA and the normal and basic lead salts of 3,5-DNBA, and later we report on a mass spectral study.

EXPERIMENTAL

Materials

3,5-DNBA
The BDH laboratory grade compound (98% purity) was used.

Normal lead salt of 3,5-DNBA (NL-3,5-DNBA)
3,5-DBNA was first converted into the sodium salt by reacting sodium hydroxide and 3,5-DNBA in 1:1 molar ratio. The sodium salt thus obtained was reacted with lead nitrate in 2:1 ratio while stirring at room temperature. The precipitated pale yellow salt was filtered off and washed with water, then with a small quantity of acetone, and dried in a desiccator.

Basic lead salt of 3,5-DNBA (BL-3,5-DNBA)
The basic salt of 3,5-DNBA was prepared by the addition of a solution of lead nitrate to sodium 3,5-dinitrobenzoate in alkaline medium at 60°C.

The precipitated reddish brown material was filtered off, washed with water and dried in a desiccator over calcium chloride. Although it is possible to obtain continuously variable stoichiometries of the basic salt, the alkali content was so adjusted as to give an approximate composition $(C_7H_3N_2O_6)_2Pb \cdot (PbO)_{0.5}$ (half basic) and $(C_7H_3N_2O_6)_2Pb \cdot PbO$ (basic).

Equipment

The following equipment was used: DSC, Perkin-Elmer DSC-2C; TG, Perkin-Elmer TGS-2; MS, JEOL DX-300 double focussing magnetic sector instrument; and SEM, JEOL 35CF model.

Experimental conditions

Differential scanning calorimetry

Prior to sample analysis, the instrument was calibrated with high purity indium. Thermograms were recorded under non-isothermal conditions. Nitrogen gas was used for purging. The samples were weighed into aluminium cups which were crimped with aluminium lids (with a pin-hole on them to allow the gaseous decomposition products to escape) using the sample cup crimper. The samples were heated at different heating rates.

Thermogravimetry

Temperature calibration was carried out using Perkalloy standard. Weight calibration was carried out using AnalaR grade copper sulphate pentahydrate. The percentage mode, which directly displays the percent weight loss vs. temperature, was used.

Mass spectrometry

Prior to sample analysis, the instrument was calibrated with perfluoro-kerosene standard. A direct insertion probe (DIP) was used for sample introduction. The sample probe was heated at a predetermined heating rate (32 K min^{-1}) and masses were recorded at 1 s scan speed in the range of 0–800 amu. Spectra were recorded at 70 eV, 100 mA ionisation current and 3 kV accelerating voltage. Chamber temperature was maintained at 250°C. The probe was heated from 50 to 350°C. An SN-23 computer (equivalent to PDP-11) was employed for acquisition and analysis of data. Spectra were recorded under low resolution (500).

Estimation of lead

The lead salt was weighed (≈ 0.30 g) accurately into a 250 ml conical flask and digested with dilute nitric acid, and the solution was diluted with distilled and deionised water after cooling to room temperature. AnalaR grade dilute sulphuric acid was run into the flask to precipitate lead as lead

sulphate. This was filtered on a G3 sintered crucible, washed with water until free from acid and finally washed with acetone. The crucible was dried at 100–110°C to constant weight and the product was weighed as $PbSO_4$.

RESULTS AND DISCUSSION

Thermal study

Thermal analysis finds extensive use in the explosives industry. Differential scanning calorimetry (DSC) is a very useful technique, and is often used to determine the thermal sensitivity/stability, heat of decomposition, phase transition temperatures and decomposition kinetics. Thermogravimetry (TG) is employed for weight loss measurements and kinetic studies. The evaluation of the thermal stability of explosives constitutes an important and growing discipline within the field of thermal analysis. The above two techniques have proved useful for the quantitative study of the thermal properties of explosives. DSC data coupled with TG data are highly useful for obtaining meaningful information. These two techniques are employed for the present study. The following samples are studied: (1) pure 3,5-dinitrobenzoic acid (3,5-DNBA); (2) the normal lead salt of 3,5-dinitrobenzoic acid (NL-3,5-DNBA); (3) the basic lead salt of 3,5-dinitrobenzoic acid (BL-3,5-DNBA).

Heat of decomposition

Heat of decomposition estimated by the DSC technique is related to the strength of the explosive. The DSC thermograms of 3,5-DNBA, NL-3,5-DNBA and BL-3,5-DNBA are displayed in Fig. 1. The sample of 3,5-DNBA melts at 483 K and then decomposes as shown in Fig. 1 (curve 3). The melting curve is not shown. The enthalpy of decomposition was estimated (195.8 J/g^{-1}). The DSC thermograms of the other two compounds (NL-3,5-DNBA and BL-3,5-DNBA) as shown in Fig. 1 (curves 1 and 2 respectively) do not show clear melting, and probably melting and decomposition may occur simultaneously or decomposition may be a solid state process. The heat of decomposition was estimated using 99.99% tin as standard and the results are shown in Table 1.

In the case of 3,5-DNBA, part of the sample underwent decomposition, and most of it escaped in the form of vapour and was deposited on the colder parts of the sample holder. The lower ΔH value may be due to this partial decomposition. In the case of the lead salts (NL-3,5-DNBA) and BL-3,5-DNBA) the decomposition was complete and the rate of decomposition was very vigorous. More sample (> 1.0 mg) and high heating rates (> 20 K min^{-1}) invariably resulted in explosion.
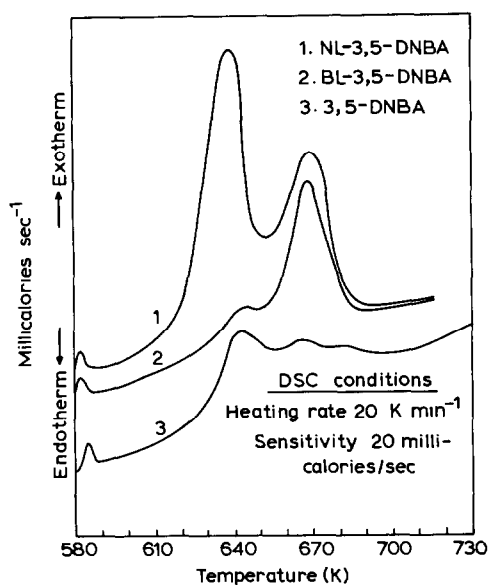
Fig. 1. DSC curves.

The weight losses for the decomposition of the above samples were recorded by using thermogravimetry (TG), and the thermograms are shown in Fig. 2. Although 3,5-DNBA showed a 75% weight loss, most of the sample was unreacted and a yellow deposit was noticed on the cold portion of the furnace tube. The sample size was restricted to < 1 mg to avoid explosion. The basic lead salt showed more explosibility compared with the normal lead salt and often exploded at a heating rate of 20 K min^{-1} or above, indicating the phenomenon of self heating at high heating rates. The lower percentage weight loss of BL-3,5-DNBA compared with that of NL-3,5-DNBA indicates the higher percentage of lead. During the decomposition, lead will be converted into non-volatile oxides.

Thermal decomposition kinetics by DSC

A popular method that has been applied extensively in the field of explosives, which was developed by Ozawa and forms the basis of the

TABLE 1

Heat of decomposition

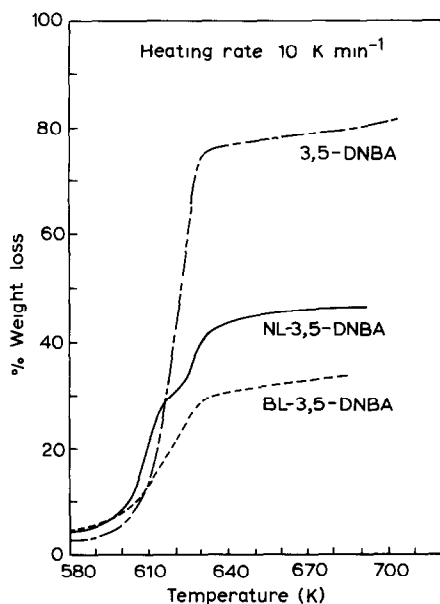| Sample	ΔH (J g^{-1})
3,5-DNBA	195.8 ± 5.0
BL-3,5-DNBA	1886.6 ± 20.0
NL-3,5-DNBA	2656.2 ± 25.0

Fig. 2. TB curves.

ASTM test method E 698, was employed for the evaluation of kinetic parameters from the non-isothermal DSC study. In a dynamic analysis the peak temperature (T_p) increases with the heating rate. This method is independent of the reaction order. The decomposition activation energy is evaluated according to the expression

$$\ln \phi = \frac{-E}{RT_p} + C$$

where ϕ is the heating rate in K min^{-1}, E is the activation energy, R is the gas constant, T_p is the peak temperature, and C is a constant. Decomposition peak temperatures are determined by heating the sample at different heating rates. In the present study, 5, 10, 20, 40 and 80 K min^{-1} heating rates were used and corresponding peak temperatures were obtained for NL-3,5-DNBA and BL-3,5-DNBA; the thermograms are displayed in Figs. 3 and 4 respectively.

Since there were no other peaks before 500 K, the sample was heated to 500 K at 80 K min^{-1} and allowed to obtain equilibrium before subjection to dynamic analysis by heating at different heating rates. The small peaks at the beginning of the thermograms are due to a sudden switch-over from the isothermal to the dynamic mode. The higher the heating rate, the bigger the peak and the greater the time taken to attain equilibrium. The normal lead salt (NL-3,5-DNBA) (Fig. 3) showed two distinct exotherms in the region 580–650 K. The first peak is more prominent than the second.
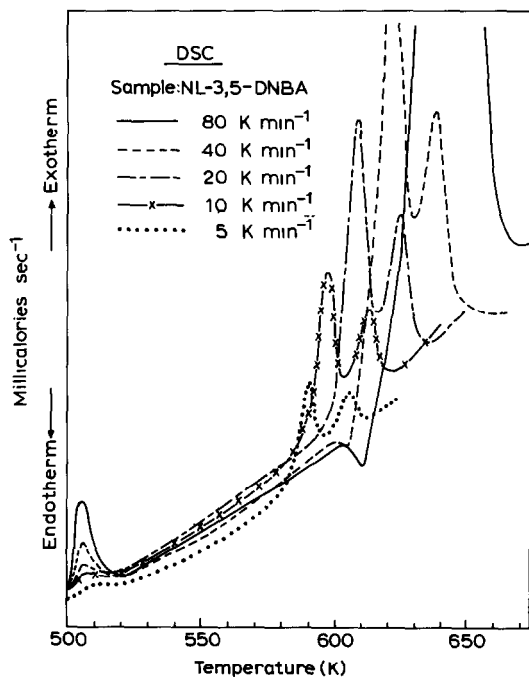
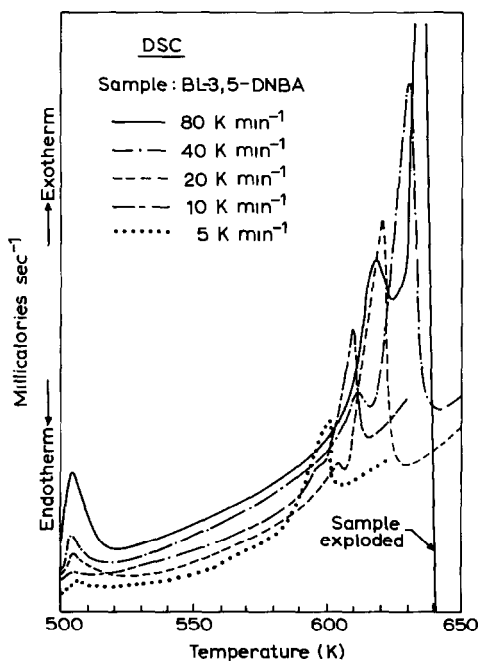Fig. 3. Effect of heating rate on the decomposition reaction.

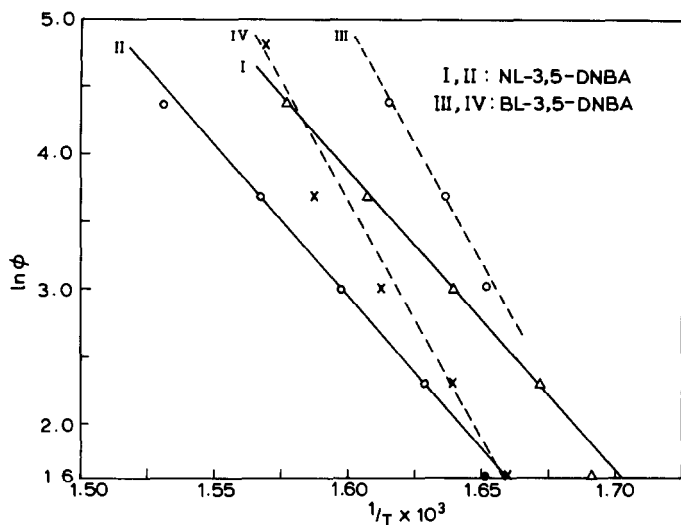Fig. 4. Effect of heating rate on the decomposition reaction.

Fig. 5. Ozawa method for DSC data analysis.

This clearly indicates two stage decomposition. It is interesting to note that the sample which showed a small endotherm preceding the exotherm, at 40 and 80 K min^{-1} heating rates showed no such endothermic peaks when thermograms were recorded at 5, 10 and 20 K min^{-1}. The endotherm may be due to the melting of the sample before undergoing decomposition, which is not noticed at lower scanning rates. This clearly shows that the decomposition is not of solid state type. The melting and decomposition are taking place simultaneously at slow heating rates and they are slightly separated at high heating rates. The basic lead salt (BL-3,5-DNBA) of dinitrobenzoic acid (Fig. 4) did not show a clear endotherm preceding decomposition, even at high heating rates. Moreover, the first peak, which was predominant in the normal salt, was not detected in thermograms recorded at 5 K min^{-1}, it appeared as a shoulder with heating at 10 K min^{-1} and was very small in thermograms recorded at higher heating rates. The second peak, which was minor in the normal lead salt, became the main peak for the basic lead salt. Many times the basic salt exploded in the DSC cell while being heated at 40 K min^{-1} and above, even though the sample size was less than 1 mg. The activation energy was calculated employing the Ozawa method [14] for normal and basic salts and the plots are shown in Fig. 5. Plots I and II correspond to peak one and peak two of the normal salt, whereas plots III and IV correspond to peak one and peak two of the basic salt. The activation energies are set out in Table 2.

It appears that the activation energy difference between peak one and peak two is very small for both salts. However, the basic salt showed a higher activation energy (275.0 kJ mol^{-1}) compared with the normal salt (187.0 kJ mol^{-1}). The reported bond energies [15] of Pb–O and C–N are

TABLE 2

Activation energy

Sample		E_{act} (kJ mol^{-1})
NL-3,5-DNBA	First peak	188.3
	Second peak	186.0
BL-3,5-DNBA	First peak	272.0
	Second peak	279.0

377.8 ± 4.2 kJ mol^{-1} and 177.8 ± 6.8 kJ mol^{-1} respectively. It can be concluded that Pb–O bond breakage may be controlling the reaction kinetics in the basic salt whereas C–NO$_2$ bond breakage may be controlling the decomposition in the normal salt.

Thermal decomposition kinetics by TG

Dynamic TG analysis was carried out on the normal and basic lead salts. The heating rates employed were 5, 10, 20 and 40 K min^{-1}. TG thermograms, showing the effect of heating rate on decomposition of the normal salt, are shown in Fig. 6. It is also clear from the sharpness of the inflection that the decomposition rate increases with increased heating rate.

Two step decomposition was noticed in the case of 5 and 10 K min^{-1} heating rates, whereas fast and single-step decomposition with a 20 K min^{-1} rate and explosion with a 40 K min^{-1} rate were observed. The oscillating balance condition was seen in the case of the thermogram recorded with 40 K min^{-1} rate at the end of decomposition curve. With all heating rates, the observed weight loss for NL-3,5-DNBA is about 40% and
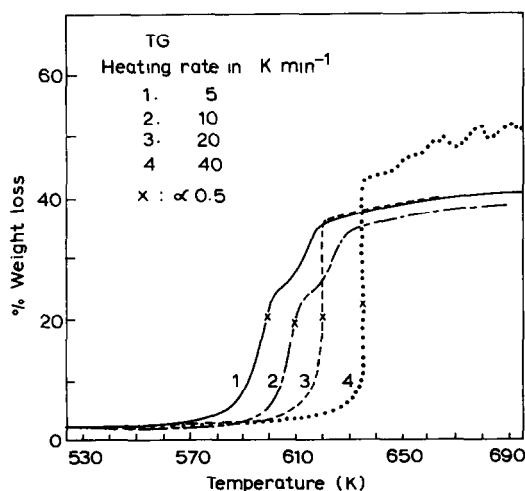

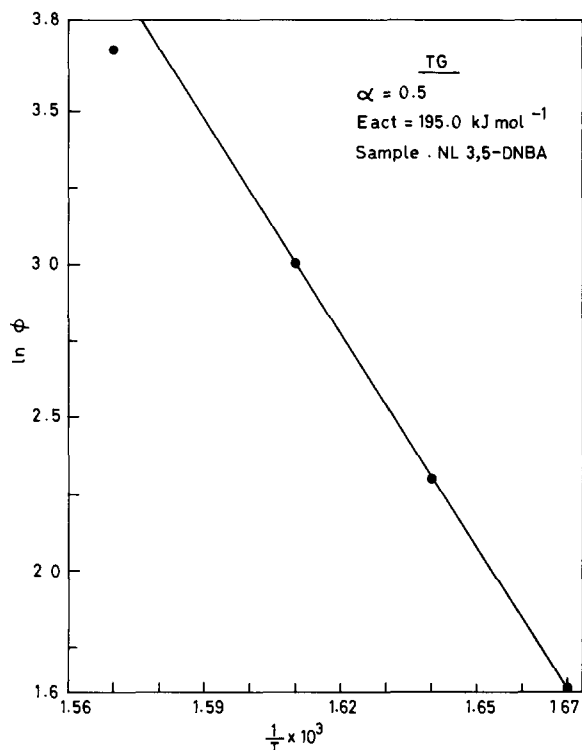Fig. 6. Effect of heating rate on the decomposition reaction.

Fig. 7. Ozawa method for TG data analysis.

that for BL-3,5-DNBA is about 30%, in good agreement with the data represented by Fig. 2.

The Ozawa method [16] was employed for handling kinetic data. This method states that the logarithm of the rate of heating ϕ has a linear relation with the reciprocal of the absolute temperature for the given conversion (α), regardless of the order of the reaction. All the thermograms were recorded using weight percent mode, and absolute temperatures, corresponding to $\alpha = 0.5$ were determined. A typical plot of $\ln \phi$ versus reciprocal temperature (for conversion 0.5) for NL-3,5-DNBA is shown in Fig. 7.

The experimental activation energy values for NL-3,5-DNBA and BL-3,5-DNBA are 195.0 and 295.0 kJ mol^{-1} respectively. These values are in fair agreement with the DSC values.

Thermal decomposition kinetics by the delay time method

The delay time (time between the start and the explosion) is a characteristic feature of an explosive. The delay times differ from sample to sample. For this purpose, a DSC instrument was used for measuring the delay time at different isothermal temperatures. The sample was crimped into alu-
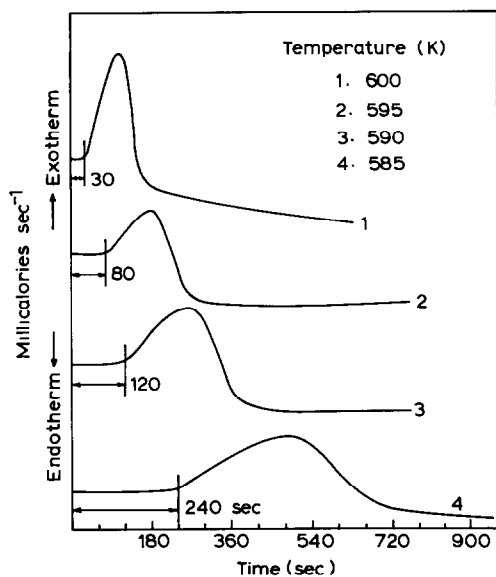
Fig. 8. Delay time measurement using DSC.

minium cups and heated rapidly at 160 K min^{-1}, and time measurement (in seconds) using a stopwatch was effected from the time the sample attained the required temperature till the time it started to decompose. The time delay (DSC) thermograms for BL-3,5-DNBA are shown in Fig. 8. A delay time method [17] was applied for this purpose and a plot of ln(delay time, s) versus the reciprocal absolute temperature gave a straight line with a slope of $-E/R$ as shown in Fig. 9. The activation energy values derived for NL-3,5-DNBA and BL-3,5-DNBA are 190.0 and 334.8 kJ mol^{-1} respectively. The latter value is slightly higher than the values obtained by TG and DSC as described earlier, and closer to the Pb–O bond energy (377.0 kJ mol^{-1}), but the former value is in fair agreement with that from the previous methods. To eliminate mass effects, the sample size was kept constant around 2.0 mg for the delay experiments.

Chemical composition of lead salts of 3,5-DNBA

It was intended to prepare lead salts of variable stoichiometries. As in the case of nitrophenols, dinitrobenzoic acid is invariably precipitated as a basic salt, even though the correct calculated molar ratios are used. Lead, being a bivalent metal ion, combines with two moles of 3,5-dinitrobenzoic acid to produce a salt of the formula $(C_7H_3N_2O_6)_2Pb$. Two basic salts were also prepared by reacting lead nitrate with sodium dinitrobenzoate and varying alkali content to obtain salts having the molecular formulae $(C_7H_3N_2O_6)_2Pb(PbO)_{0.5}$ and $(C_7H_3N_2O_6)_2Pb \cdot PbO$ respectively. The
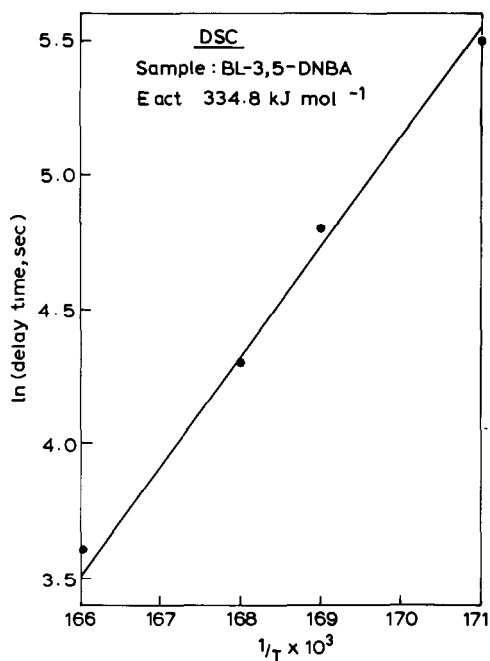
Fig. 9. Delay time method.

structures are displayed in Scheme 1. The lead content was estimated and the data are shown in Table 3.

The experimental lead value obtained for the above salts is slightly more than the theoretical value, indicating that the salts are more basic than expected. The salts NL-3,5-DNBA and BL-3,5-DNBA, which have been studied in detail and are referred to in the text, conform to the composition of samples 1 and 3 respectively.
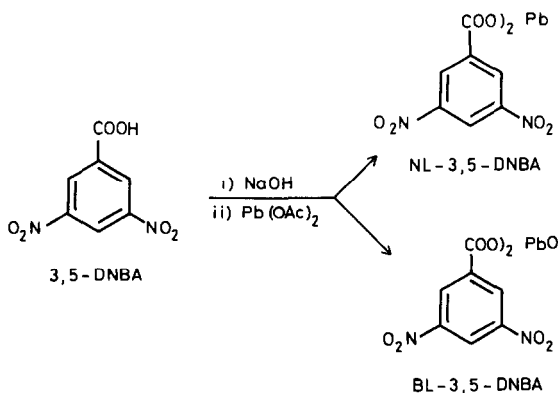
Scheme 1.

TABLE 3

Compositions of lead salts

| Sample | Expected formula | Lead content (%) | |
		Expected	Experimental
1 Normal	$(C_7H_3N_2O_6)_2Pb$	32.9	36.5
2 Half basic	$(C_7H_3N_2O_6)_2Pb(PbO)_{0.5}$	41.9	42.9
3 Basic	$(C_7H_3N_2O_6)_2Pb \cdot PbO$	48.6	50.1

Thermal sensitivity

The above samples 1, 2 and 3 were studied for their thermal sensitivity. All the samples were heated at 20 K min^{-1} in DSC and the thermograms are shown in Fig. 10. It is very interesting to note that the thermal sensitivity increases with increased basicity. All the samples show two stage decomposition. Sample 1, which is supposed to be neutral (normal), showed more first stage decomposition (I) than second stage decomposition (II). In sample 2, which is half basic, second stage decomposition predominates over first stage decomposition. First stage decomposition is almost negligible in sample 3 compared with second stage decomposition. Basicity affects the thermal sensitivity by about 20 K. Although there is a marginal difference between half basic and basic with regard to onset temperature, a clear shift in the maximum temperature of the peak is observed (see Table
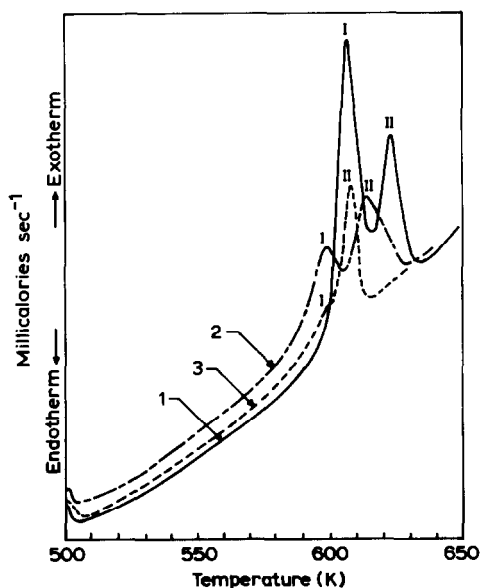

Fig. 10. Effect of basicity on the thermal sensitivity. Curve 1, normal; curve 2, half basic; curve 3, basic.

TABLE 4

Thermal sensitivity of lead salts of 3,5-DNBA

Sample	Onset temperature (K)	Peak temperature (K)
Normal	596.0	625.0
Half basic	590.0	610.0
Basic	589.0	605.0

4). The increase in basicity not only increases the thermal sensitivity of the lead salts but also minimises the first stage decomposition.

Microscopic examination

Crystal morphology of an explosive plays a very important role from the application point of view, as well as in terms of explosive sensitivity. Temperature, stirring, rate of addition and pH contribute to the crystal habit. Both normal (NL-3,5-DNBA) and basic (BL-3,5-DNBA) salts were examined under an optical microscope and showed the appearance of
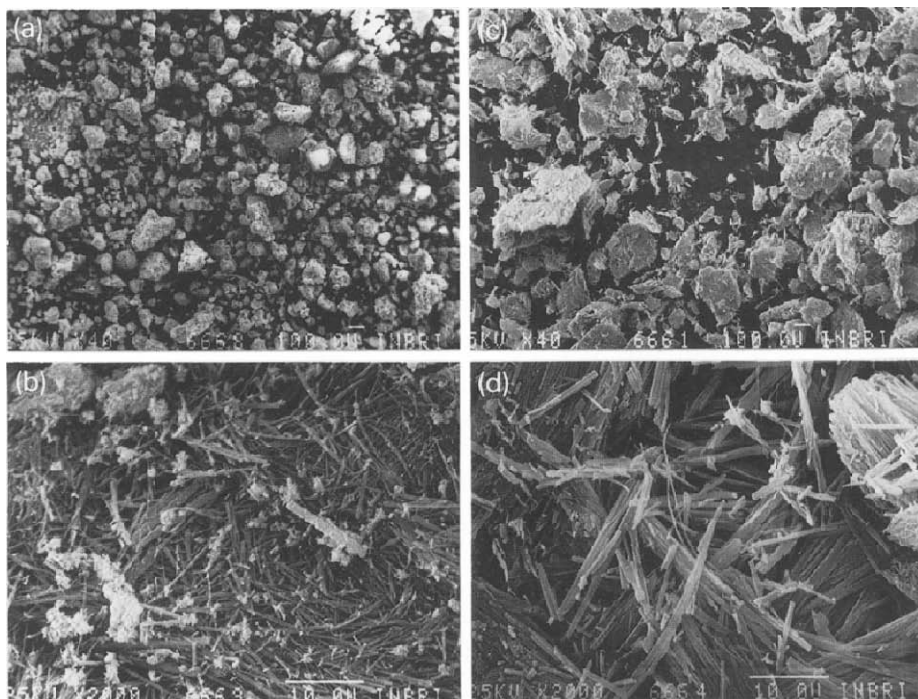

Fig. 11. Scanning electron micrographs. (a) BL-3,5-DNBA (original magnification ×40); (b) BL-3,5-DNBA (original magnification ×2000); (c) NL-3,5-DNBA (original magnification × 40); (d) NL-3,5-DNBA (original magnification × 2000).
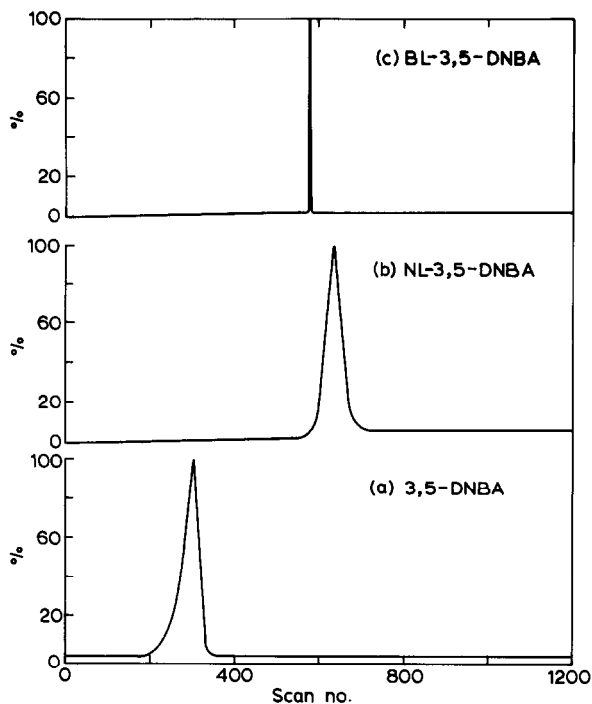
Fig. 12. TIC chromatograms.

globular agglomerates. The same samples were examined under a scanning electron microscope (SEM) to study the shape and size of the crystals. The globular crystals as seen under the optical microscope are in fact an aggregate of thousands of very thin needle-like crystals. The SEM photographs of samples of NL-3,5-DNBA and BL-3,5-DNBA are shown in Fig. 11. The low-original-magnification ($\times 40$) pictures are similar to those seen under an optical microscope where the original-magnification $\times 2000$ pictures indicate clear thin needle-like crystals. The crystal size of the NL-3,5-DNBA sample (width 0.3–0.7 μm, length 10–20 μm) is bigger than that of the BL-3,5-DNBA sample (width 0.2–0.4 μm, length 10–15 μm). Because of this needle-like nature, the crystals were not free flowing.

Mass spectral study

The total ion current (TIC) chromatograms of 3,5-DNBA, NL-3,5-DNBA and BL-3,5-DNBA are shown in Fig. 12. All the samples were heated at a constant rate of 32°C min^{-1}. From the TIC of 3,5-DNBA (Fig. 12(a)) it appears that the sample vaporises first and then undergoes decomposition under electron impact conditions. The TIC chromatogram spans over scan numbers 200–350 (156–186°C). The mass spectra recorded throughout the scanning range were identical (see Fig. 13(a)). In all cases, the parent ion
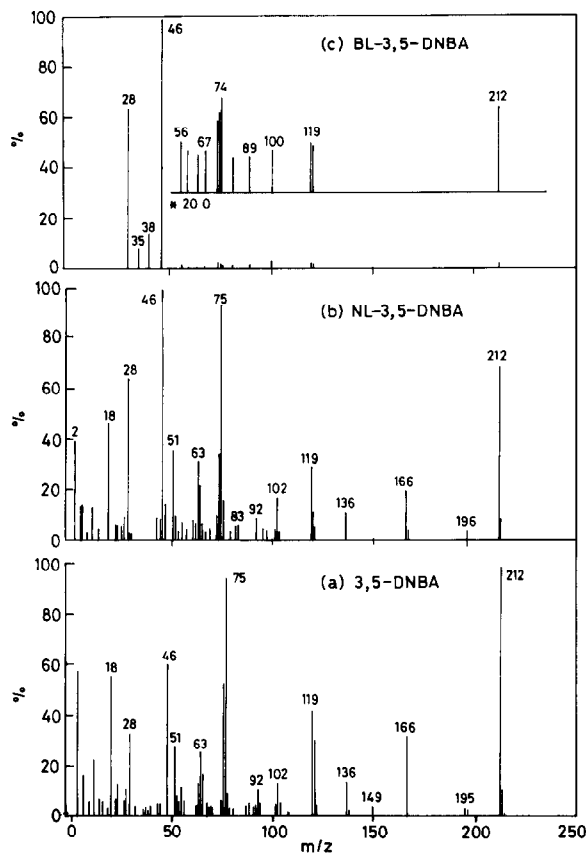
Fig. 13. Mass spectra.

(M^+) is the base peak; other prominent ions are shown in Table 5. The fragmentation pathways are shown in Scheme 2.
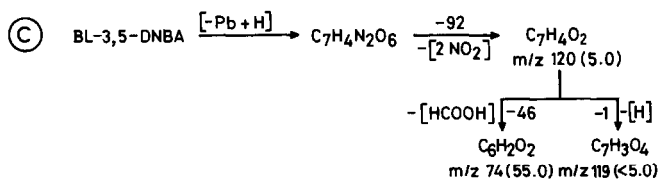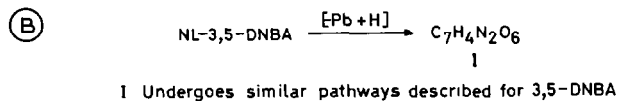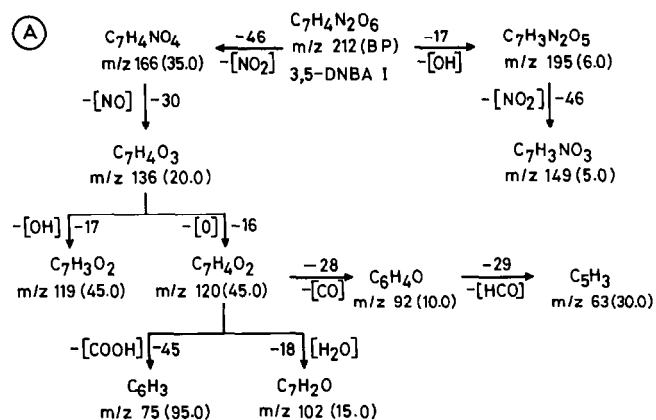
The TIC chromatogram of NL-3,5-DNBA presented in Fig. 12(b) shows no ion current up to scan no. 570 and the ion current spreads over scans no. 580–700. The mass spectra recorded throughout the scanning range were identical. The base peak was found to be 46, which is due to the NO_2 fragment. The highest mass fragment observed was 212 (M-Pb + H). The formation of this type of ion is in accordance with our previous study on nitrophenols. The number of fragments observed in the mass range of 100–212 is few compared with the parent molecule 3,5-DNBA (see Fig. 13(b)). This type of pattern is indicative of the existence of unstable species which undergo further rapid fragmentation.

The TIC chromatogram of BL-3,5-DNBA presented in Fig. 12(c) shows a very interesting pattern. Up to scan no. 587 and after scan no. 589, no ion current can be noticed. The total ion current is confined to two scans and indicates sample explosion. Such a pattern is also observed for lead dinitroresorcinol [12], lead dinitrophenol and lead picramate [13]. The mass

TABLE 5

Species evolved from fragmentation of 3,5-DNBA and its lead salts

3,5-DNBA		NL-3,5-DNBA		BL-3,5-DNBA	
m/z	% abundance	m/z	% abundance	m/z	% abundance
212	b.p. [a]	212	75.0	212	< 5.0
195	6.0	196	5.0	120	< 5.0
166	35.0	166	20.0	74	< 5.0
149	5.0	136	15.0	56	< 5.0
136	20.0	119	30.0	46	b.p. [a]
119	45.0	102	20.0	38	15.0
102	15.0	92	10.0	35	5.0
92	10.0	75	90.0	28	62.0
75	96.0	63	30.0		
63	30.0	51	35.0		
51	30.0	46	b.p. [a]		
47	60.0	28	65.0		
42	5.0	18	50.0		
28	35.0				
18	60.0				

[a] Base peak.

(A) $C_7H_4NO_4$ m/z 166 (35.0) ←$\frac{-46}{-[NO_2]}$— $C_7H_4N_2O_6$ m/z 212 (BP) 3,5-DNBA I —$\frac{-17}{-[OH]}$→ $C_7H_3N_2O_5$ m/z 195 (6.0)

-[NO] | -30

-[NO_2] | -46

$C_7H_4O_3$ m/z 136 (20.0)

$C_7H_3NO_3$ m/z 149 (5.0)

-[OH] | -17   -[O] | -16

$C_7H_3O_2$ m/z 119 (45.0) $C_7H_4O_2$ m/z 120 (45.0) —$\frac{-28}{-[CO]}$→ C_6H_4O m/z 92 (10.0) —$\frac{-29}{-[HCO]}$→ C_5H_3 m/z 63 (30.0)

-[COOH] | -45   -18 | [H_2O]

C_6H_3 m/z 75 (95.0) C_7H_2O m/z 102 (15.0)

(B) NL-3,5-DNBA —[Pb+H]→ $C_7H_4N_2O_6$ I

I Undergoes similar pathways described for 3,5-DNBA

(C) BL-3,5-DNBA —[-Pb+H]→ $C_7H_4N_2O_6$ —$\frac{-92}{-[2NO_2]}$→ $C_7H_4O_2$ m/z 120 (5.0)

-[HCOOH] | -46   -1 | -[H]

$C_6H_2O_2$ m/z 74 (55.0) $C_7H_3O_4$ m/z 119 (<5.0)

Scheme 2.

spectrum recorded at scan no. 588 is displayed in Fig. 13(c). The low abundance of fragment ions between masses 50 and 212 and the very few fragments are an indication of the formation of unstable fragments as a result of explosion. Unlike the findings in our previous observation, the masses due to isotopes of Pb^{2+}, namely 206, 207 and 208, and adduct ions with M^+ ($M + NO_2$ and $M + NO$) were totally absent. The ion due to 3,5-dinitrobenzoate (m/z 211) is also absent. In this case also, as with NL-3,5-DNBA, the base peak was 46 (due to NO_2). Interestingly, fragment ion 46 is absent in 3,5-DNBA.

The mass spectrum of NL-3,5-DNBA more or less resembles the mass spectrum of 3,5-DNBA, whereas the mass spectrum of BL-3,5-DNBA is totally different. The fragments like those at mass 120, 74 and 38 present in BL-3,5-DNBA are absent in the mass spectrum of the other two samples. The mass 51 fragment present in 3,5-DNBA and NL-3,5-DNBA is absent in BL-3,5-DNBA. It should be realised that the sample temperature during explosive decomposition in a mass spectrometer will be several hundred degrees above the temperature of analysis, and this may produce fragments of unusual origin.

CONCLUSIONS

The thermal sensitivity of lead salts of 3,5-DNBA increases with increase in basicity.

The kinetics of decomposition indicate two different types of mechanism: Pb–O bond breakage controls the decomposition of the basic salt, whereas $C–NO_2$ bond breakage occurs in the normal salt.

A mass spectral study indicated some unexpected ions due to explosion.

REFERENCES

1 W. Brun, US Patent 1,971,029, 1934; Chem. Abstr., 28 (1934) 6314.
2 W. Brun, US Patent 1,991,730, 1935; Chem. Abstr., 29 (1935) 2360.
3 W. Brun, US Patent 1,887,919, 1932; Chem. Abstr., 27 (1933) 1513.
4 P.H. Burdett and G.M. Calhoun, US Patent 2,345,868 1944; Chem. Abstr., 38 (1944) 4806.
5 W. Friederich, Br. Patent 193,830, 1921.
6 A.E. Fogelzang et al. Tr. Mosk Khim. Tekhnol Inst. im. D.I. Mendeleeva, 112 (1980) 70; Chem. Abstr., 99 (1983) 40670u.

7 V. Kaderabek, V. Koudelkova and V. Nymsova, Chem. Prum., 30(5), (1980) 238–42 Chem. Abstr., 93 (1980) 149529 g.

8 J. Frank and J. Pour, Sb. ved. Pr., Vys. S. K. Chemiko technol., Pardubice, No. 25, 1971, 41–51; Chem. Abstr., 75 (1971) 110004k.

9 H.G. Dorsett and J. Nagy, Rep. U.S. Invest. Bur. Mines, RI-7132, 1968.

10 J.H. Bowie, Org. Mass Spectrom., 5(8) (1971) 945.

11 M.J. Welch, R. Sams and E. White, Anal. Chem., 58(4) (1986) 890.

12 S.R. Yoganarasimhan, G. Om Reddy and S. Achar, Propellants, Explos., Pyrotechn., 14 (1989) 234.

13 S.R. Yoganarasimhan, G. Om Reddy and Sudhir Achar, J. Energ. Mater., accepted for publication.

14 T. Ozawa, Bull. Chem. Soc. Jpn., 38 (1965) 1881.

15 CRC Handbook of Chemistry and Physics, 60th edn., 1979–1980, CRC Press, Boca Raton, FL.

16 T. Ozawa, J. Therm. Anal., 2 (1970) 301.

17 A.J.B. Robertson, Trans. Faraday Soc., 44 (1948) 977.